JTTEE5: 4:175-178

Comparative Study of the Structure of Gas-Stabilized and Water-Stabilized Plasma Jets

S. Raghu, G. Goutevenier, and R. Gansert

The near-field structures of a gas-stabilized plasma jet and a water-stabilized plasma jet were investigated using a nano-pulsed laser probe and stroboscopic focusing schlieren techniques. The high exit temperatures of the gas caused laminar flow conditions at the exit of the jet, producing instability waves in the region. Significant heat conduction to the ambient fluid and volumetric expansion of the ambient gases in the near-field were observed in the schlieren images of these jets. Considerable asymmetry in the mixing and entrainment region of the water-stabilized plasma jet was also visible, whereas no significant asymmetry occurred in the luminous core of the jet. The particles injected into the plasma jet, which were visualized by the pulsed-laser technique, were confined to a narrow central core of the jet in the near-field of the jet. The combination of the two visualization techniques used in the present study allowed nonintrusive monitoring of the plasma spray process in an effort to enhance the quality of the processed deposits.

1. Introduction

PLASMA jets are used to deposit protective coatings on substrates and in near-net or net-shape manufacturing. These high-velocity jets (with exit velocities of up to 1000 m/s) have exit temperatures greater than 10,000 K in the case of gas-stabilized plasma (GSP) jets (Ref 1, 2) and up to 30,000 K in water-stabilized plasma (WSP) jets (Ref 3). Particles of the desired coating material are injected into the jet either close to the nozzle exit or within the nozzle chamber. Although the basic coating principle is the same for both types of jets, the construction of the plasma guns is different (see Section 2). A comparative study of the structure of the plasma jets produced by the two types of guns was conducted in order to relate jet properties to the nature of the resulting coating.

Flow visualization studies have aided understanding of the structure of flow fields and the important processing parameters that affect both flow and the transported particles. An example is the discovery of the large-scale structures in turbulent shear flows (Ref 4). A more extensive collection of various flow fields visualized using different techniques can be found in Ref 5. The present work was prompted by the impact of flow visualization on the study of fluid mechanics and plasma jet dynamics.

Plasma jets have been visualized using a laser probe system (Ref 6, 7) and pulsed schlieren and shadowgraph techniques (Ref 2). The laser probe system uses narrow band-pass filters to reduce the intensity of light entering a charge coupled device (CCD) camera with 50 ns to 1 μs shutter speeds. This allows visualization of the luminous central part of the jet, which extends a few diameters downstream of the exit corresponding to the jet core region. Due to entrainment and mixing of the jet with colder ambient fluid, both the outer shear layer of the jet and the downstream flow field are at a lower temperature and cannot be visualized by direct observation of the plasma flame. In regular pulsed schlieren visualization, such as that reported by Fincke et al. (Ref 2), the edges of the jet are clearly visible, but the near field is overwhelmed by the plasma glow, masking the details of the jet structure. This technique also averages the density variations along the optical path and, in addition to the density variations in the jet, the convection/recirculation currents in the enclosure affect the quality of the visualization process. The presence of dust in the enclosure creates additional problems. The dust fogs the lenses and rapidly deteriorates the quality of the schlieren images. This prompted the use, in the present work, of the focusing schlieren technique in conjunction with a laser probe system to obtain details of the jet structure.

The focusing schlieren technique (Ref 8, 9) has not previously been used to visualize high-temperature glowing jet fields. Briefly, the technique consists of a diffused light source and a pair of grids (a source grid and a cutoff grid), between which is the required flow field with varying refractive indices. The source grid acts as multiple light sources, and the cutoff grid acts as multiple knife edges. The image formed on a screen at a given distance behind the knife edge is the superposition of all the images refracted from a single plane of the flow field in which there is a refractive index gradient. The focusing schlieren method does not require a point light source; any source of bright light can be used in the setup. Hence, ordinary strobe lights can be used instead of a more expensive laser source to obtain instantaneous pictures of the flow field.

Keywords: jet spreading, plasma jets, schlieren technique, water-stabilized plasma

S. Raghu and **G. Goutevenier,** Department of Mechanical Engineering, State University of New York, Stony Brook, NY 11794; **R. Gansert,** Department of Materials Science and Engineering, State University of New York, Stony Brook, NY 11794

2. Experimental Arrangement

A commercially available METCO 3MB, Metco Perkin-Elmer, Westbury, NY, GSP gun and a PAL 160 (Institute of Plasma Physics, Prague Czech Republic) WSP gun were used. Both guns have a nozzle exit diameter of 6 mm and thus alloy com-

parative studies to be made. The GSP gun has a central cathode, with the nozzle wall acting as the anode (see, for example, Ref 10), whereas the WSP gun has an external rotating anode at the exit of the nozzle (Ref 3). The GSP jet was operated at an argon flow rate of 40 L/min, and the average values of current and voltage were 450 A and 60 V, respectively (about 27 kW). The WSP jet was operated at an arc power of about 126 kW (at about 290 to 300 V and 400 to 410 A).

For the GSP jet, 50 to 60 μm aluminum particles with argon as the carrier gas were injected normal to the jet axis from a 5 mm ID tube placed at $x = 20$ mm, where x is the downstream distance from the exit of the jet ($\chi/d \approx 3$). For the WSP jet, iron particles with a maximum size of 150 μm (100 mesh) and air as the carrier gas were injected at $x = 70$ mm ($\chi/d \approx 12$) at an angle of 56° with respect to the jet axis and in the downstream direction of the jet. The centerline velocity of the carrier gas at the exit of the particle seeding tube was approximately 70 m/s for both types of sprays. The momentum flux ratio of the particle seeding jet with respect to the plasma jet, defined as $(\rho U^2)_{\text{seedingjet}}/(\rho U^2)_{\text{plasma jet}}$ (where ρ is the density of the gas and U is the velocity at the exit of the nozzle), was in the range of 0.10 to 0.20 for a plasma exit velocity of 1000 m/s. The particle feed rates were approximately 10 kg/h for the GSP jet and 40 kg/h for the WSP jet.

Details of the focusing schlieren arrangement are shown in Fig. 1. The grids were made from a computer-generated pattern and differed from that used in Ref 9 in that the cutoff grid, rather than being a negative of the source grid, consisted of an array of very narrow slits proportionately reduced in size in relation to the focal length of the lens. The light blockage ratio obtained from the ratio of the slit width to slit spacing of the cutoff grid was 94%. Thus, the cutoff grid served two purposes: it eliminated the unwanted glow from the plasma jet and provided details of the plasma jet in one plane. The light source was an EG&G strobe light with a flash duration of 20 to 40 μs, a frequency range of 1 to 120 Hz, and a maximum power of 12 J per pulse. The strobe light was synchronized with a CCD camera operating at the same speed (30 frames per second) with a shutter speed of 100 μs. This optical arrangement allowed the glow from a 1000 W filament bulb placed in the optical path to be completely masked while the convective currents around the bulb were clearly visible on the screen. The images were video-recorded and subsequently processed.

The laser probe system (Ref 7) consisted of two pulsed nitrogen lasers (Model LN-300) that produced pulsed outputs in the ultraviolet regime with wavelengths of 337 nm. The maximum output of the laser was 250 μJ per pulse, and the pulse width was 5 ns. The interval between the pulses could be varied between 1 μs and 8 ms. The beams of light illuminated the injected particles and were viewed through a CCD camera with a narrow band-pass filter (337 nm) and shutter speeds of 70 ns to 5 μs. In addition to the scattered light from the particles, the luminous core of the plasma jet with ultraviolet emission at the above wavelength could also be visualized using this system.

In the present study, attention was confined to the "near-field" of the jet—that is, the region where rapid development of the jet structure takes place, beginning at the exit of the nozzle and extending up to 6 to 8 diameters downstream of the exit. An understanding of the dynamics of this region is essential in order to optimize process parameters (such as the location and direction of particle injection) and to devise techniques to control mixing of the jet with ambient fluid.

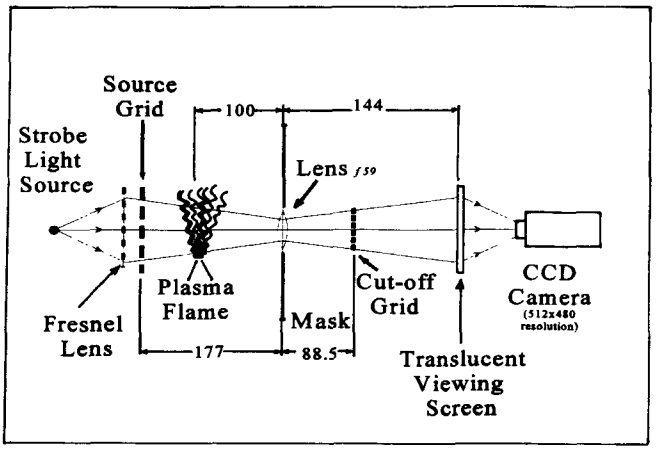

Fig. 1 Focusing schlieren arrangement. All dimensions are in centimeters.

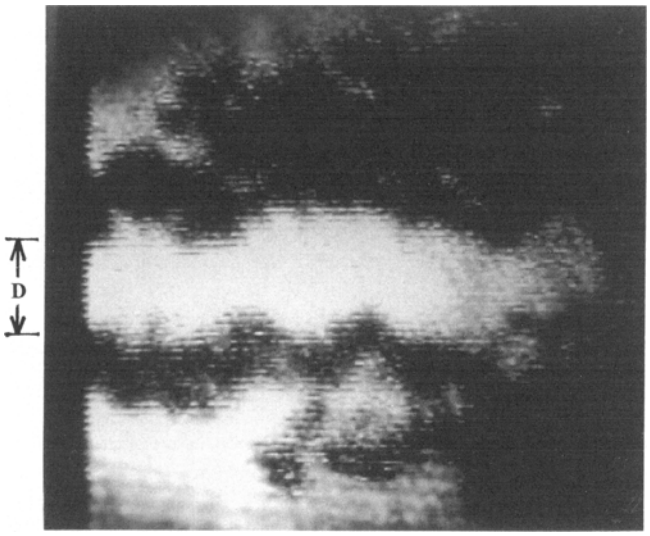

Fig. 2(a) Exit region of the GSP jet showing instability waves in the luminous jet core. The argon flow rate was 40 L/min, at 550 V and 60 A. The horizontal lines are remnants of the cutoff grid positioned to eliminate the plasma glow. The flow is from left to right.

3. Results and Discussion

Figure 2(a) shows a schlieren image of the near-exit region of the GSP jet under the operating conditions previously outlined. The luminous jet is initially laminar, and instability waves form within 1 or 2 diameters downstream of the exit. The instability wavelength is on the order of the jet diameter, and, due to the growth of these into large-scale coherent vortical structures and the associated entrainment, the ambient fluid is drawn toward the center of the jet. The luminosity disappears downstream of this region ($x/d > 5$), indicating that the entrained colder fluid has reached the centerline of the jet. Thus, the high-temperature plasma flame in the core of the jet is quenched at this point and

Fig. 2(b) Near-field of the GSP jet showing the large region of ambient fluid affected by the plasma jet. Same operating conditions as in Fig. 2(a).

the centerline temperature drops rapidly beyond this distance, which is in agreement with the measurements of Pfender et al. (Ref 1). The length of the luminous core fluctuated from 5 to 7 diameters downstream from the jet exit, indicating random axial locations where the ambient fluid reached the center of the jet. This fluctuation in the length of the luminous core, referred to as "surging," and the lateral or whipping motion of the tip of the flame, also observed in our experiments, have been attributed to arc instabilities in the plasma guns (Ref 11, 12). Farther downstream, these large-scale vortical structures break down into smaller structures, thus causing transition to turbulence.

The visual spread of the jet (Fig. 2b) is significantly larger than that of an isothermal turbulent jet. The half-angle of the jet spread is about 20° and is symmetric with respect to the jet axis. This large spreading of the jet, as visualized by the schlieren method, requires further study. The instability waves in the luminous region of the jet indicate initially laminar conditions at the jet exit; therefore, only a small amount of entrainment and mixing in the near-region of the jet can be expected. However, the surrounding fluid in the exit region that appears turbulent extends radially up to a distance of 1 to 2 diameters from the edge of the luminous zone. Observation of the video pictures indicates that a sheath of slow-moving outer fluid (about 0.5 diameters thick at the exit of the jet), heated by thermal conduction from the hot jet, surrounds the exit region and is drawn into the entrainment field downstream, thus giving the illusion of a large spreading of the jet (this also was reported in Ref 1). This observation is supported by the fact that the viscosity and thermal conductivity of the air increase by a large magnitude from room temperature to the exit temperature of the plasma jet, causing laminar flow conditions at the exit and high heat conduction in the edges of the jet. Such laminarization of the shear layer and heat conduction to the outer fluid have been observed in diffusion flames by Roquemore et al. (Ref 13), who found that the flow field of this outer fluid significantly affects the inner jet. The role of the outer fluid in plasma jet dynamics has not yet been determined.

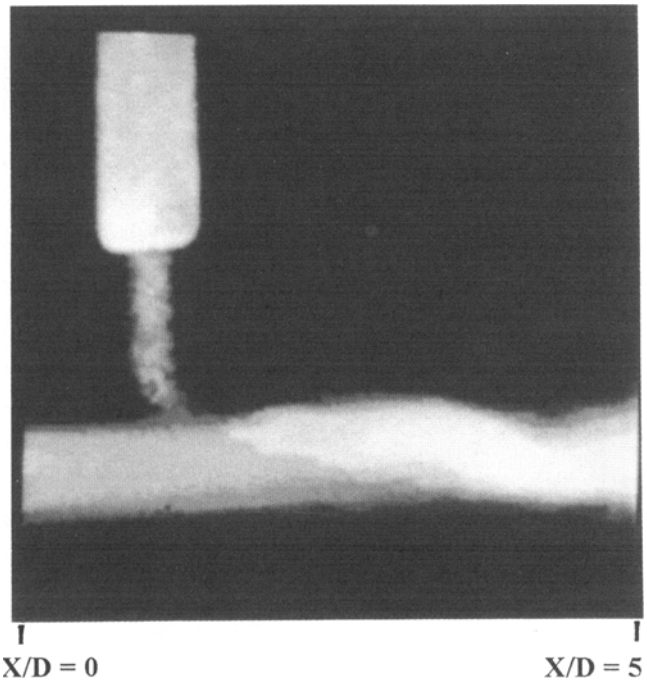

Fig. 2(c) Particle streaks in the GSP jet visualized using the laser probe. Same operating conditions as in Fig. 2(a).

Figure 2(c) shows laser probe visualization of the luminous core of the GSP jet and the particles that were externally injected as described in Section 2 of this paper. The particles are drawn into a thin core not significantly larger than the exit diameter of the jet, which remains this size even at 10 diameters downstream of the jet exit. Due to partial evaporation of the particles, a bright vapor cloud is seen about 20 mm downstream of the particle injection. Comparison of Fig. 2(c) and 2(b) confirms the observation that the high-momentum plasma jet is confined to a small central region and that the heating and volumetric expansion of the ambient air causes the appearance of a large pseudo-spread rate in the schlieren images of the jet.

Figure 3(a) shows the structure of a WSP jet visualized using the focusing schlieren. The structure of the luminous core appears very similar to that of the GSP jet and extends up to 8 diameters downstream of the exit. The longer length of the luminous core is due to the larger power input to the WSP jet (126 kW) compared to the GSP jet (27 kW). Also, considerable asymmetry in the spread of the surrounding fluid is apparent. The spread angle on the anode (bottom) side is one and a half times (or 30°) the spread on the opposite side, suggesting that the jet attaches to the rotating anode surface and then separates from the edge of the anode. Studies are under way to determine the effect of such asymmetry on deposition characteristics.

Figure 3(b) shows the luminous core and the particles that were injected externally into the plasma jet. The particles remain in a thin column until they reach the luminous core of the jet at a distance approximately 8 diameters downstream of the exit. Thus, the main momentum-carrying fluid in the near-field corresponds to the luminous core of the jet, although the schlieren images indicate a large spread of the jet.

Comparison of the schlieren images of the GSP and WSP jets shows that the WSP has a larger spread angle, as measured by the visual boundaries of the jets. The schlieren images also indi-

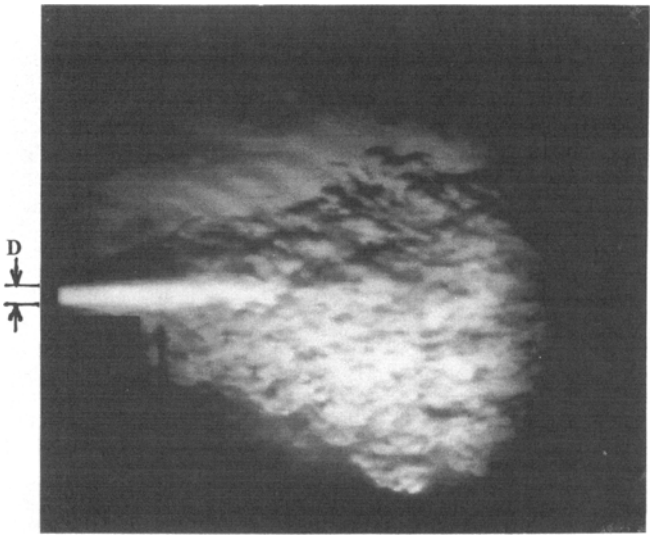

Fig. 3(a) Schlieren image of the WSP jet with an arc power of 160 kW

Fig. 3(b) Luminous region of the WSP jet and the particle injection visualized using the laser probe

cate considerable asymmetry in the spread of the WSP jet. However, as pointed out earlier, these spread angles do not distinguish between the actual momentum-carrying plasma jet and the outer fluid that is heated by conduction. The central luminous core, corresponding to the momentum-carrying fluid in the near-field region, does not show significant spread or large asymmetry for the WSP gun. A higher degree of unsteadiness (i.e., larger fluctuations in the length of the luminous core as well as larger amplitudes of flapping) was observed in the WSP luminous core.

4. Conclusion

The stroboscopic focusing schlieren technique and the laser probe system provide a nonintrusive method of monitoring the thermal spray process in order to obtain a good coating. The schlieren images provide details of the entire plasma jet (the luminous core and the mixing region), and the laser probe visualizes the particles in the plasma jet.

Laminar flow conditions result from the intense heat of the jet, and instability waves occur at the exit of the jet. The GSP jet is symmetric in the entrainment and mixing region, whereas the WSP jet shows significant asymmetry due to the external, rotating anode. In both cases, the visual spread of the jets is much larger compared with that of an isothermal turbulent jet. The particle distributions in the near-fields of the jets, however, do not indicate large differences in trajectories. As visualized by the schlieren technique, in both GSP and WSP jets the particles penetrate directly into the luminous jet core without being affected by the large thermal layer.

Acknowledgment

This work was supported by the National Science Foundation under grants NSF-DDM-9215846 and NSF-MSS-9311053 from the Division of Design, Manufacture and Industrial Innovation and the Division of Civil and Mechanical Structures, respectively.

References

1. E. Pfender, J. Fincke, and R. Spores, Entrainment of Cold Gas into Thermal Plasma Jets, *Plasma Chem. Plasma Process.*, Vol 11 (No. 4), 1991, p 529-543
2. J.R. Fincke, W.D. Swank, and D.C. Haggard, Entrainment and Demixing in Subsonic Argon/Helium Thermal Plasma Jets, *J. Therm. Spray Technol.*, Vol 2 (No. 4), 1993, p 345-350
3. P. Chraska and M. Hrabovsky, An Overview of Water Stabilized Plasma Guns and Their Applications, *Thermal Spray: International Advances in Coatings Technology*, C.C. Berndt, Ed., ASM International, 1992, p 81-85
4. G. Brown and A. Roshko, On Density Effects and Large Structures in Turbulent Mixing Layers, *J. Fluid Mech.*, Vol 64 (No. 4), 1974, p 775-816
5. M. Van Dyke, Ed., *An Album of Fluid Motion*, Parabolic Press, 1982
6. S. Malmberg, J. Heberlein, and E. Pfender, DC Plasma Jet Structure and Particle Velocities During Spraying, *Thermal Spray Conference*, German Welding Society, Dusseldorf, 1993, p 40-44
7. J. Agapakis and T. Hoffman, Real-Time Imaging for Thermal Spray Process Development and Control, *J. Therm. Spray Technol.*, Vol 1 (No. 1), 1992, p 19-25
8. R.A. Burton, A Modified Schlieren Apparatus for Large Areas of Field, *J. Opt. Soc. Am.*, Vol 39, 1949, p 907-908
9. L.M. Weinstein, An Improved Large-Field Focusing Schlieren System, American Institute of Aeronautics and Astronautics, AIAA-91-0567, *29th Aerospace Sciences Meeting*, Reno, NV, 1991
10. H. Herman, Plasma-Sprayed Coatings, *Sci. Am.*, Vol 256, 1988, p 113-117
11. S. Russ, E. Pfender, and J. Heberlein, Anode Arc Attachment Control Using Boundary Layer Bleed Holes, *Thermal Spray Coatings: Research, Design and Applications*, C.C. Berndt and T.F. Bernecki, Ed., ASM International, 1993, p 97-103
12. S. Russ, P.J. Strykowsky, and E. Pfender, Mixing in Plasma and Low Density Jets, *Exp. Fluids*, Vol 16, 1994, p 297-307
13. W.M. Roquemore, L.-D. Chen, J.P. Seaba, P.S. Tschen, L.P. Goss, and D.D. Trump, Jet Diffusion Flame Transition to Turbulence, *Phys. Fluids*, Vol 30, 1987, p 2600